ResearchGate

See discussions, stats, and author profiles for this publication at: https://www.researchgate.net/publication/259313948

Spatial Arrangement of Organic Compounds on a Model Mineral Surface: Implications for Soil Organic Matter Stabilization

ARTICLE *in* ENVIRONMENTAL SCIENCE & TECHNOLOGY · DECEMBER 2013

Impact Factor: 5.33 · DOI: 10.1021/es403430k · Source: PubMed

CITATIONS
4

READS
153

7 AUTHORS, INCLUDING:

Sindhu Jagadamma
Oak Ridge National Laboratory
23 PUBLICATIONS **258** CITATIONS
SEE PROFILE

Bradley S Lokitz
Oak Ridge National Laboratory
40 PUBLICATIONS **1,499** CITATIONS
SEE PROFILE

Valeria Lauter
Oak Ridge National Laboratory
118 PUBLICATIONS **706** CITATIONS
SEE PROFILE

Melanie Mayes
Oak Ridge National Laboratory
72 PUBLICATIONS **681** CITATIONS
SEE PROFILE

Available from: Melanie Mayes
Retrieved on: 01 February 2016

Environmental Science & Technology

Article

pubs.acs.org/est

Spatial Arrangement of Organic Compounds on a Model Mineral Surface: Implications for Soil Organic Matter Stabilization

Loukas Petridis,*[,†] Haile Ambaye,[‡] Sindhu Jagadamma,[§,∥] S. Michael Kilbey, II,[⊥,#] Bradley S. Lokitz,[⊥] Valeria Lauter,[▽] and Melanie Mayes[§,∥]

[†]Center for Molecular Biophysics, Oak Ridge National Laboratory, Oak Ridge, Tennessee 37831, United States

[‡]Research Accelerator Division, Oak Ridge National Laboratory, Oak Ridge, Tennessee 37831, United States

[§]Environmental Sciences Division, Oak Ridge National Laboratory, Oak Ridge, Tennessee 37831, United States

[∥]Climate Change Science Institute, Oak Ridge National Laboratory, Oak Ridge, Tennessee 37831, United States

[⊥]Center for Nanophase Materials Sciences, Oak Ridge National Laboratory, Oak Ridge, Tennessee 37831, United States

[#]Department of Chemistry and Chemical & Biomolecular Engineering, University of Tennessee, Knoxville Tennessee 37996, United States

[▽]Quantum Condensed Matter Division, Oak Ridge National Laboratory, Oak Ridge, Tennessee 37831, United States

Supporting Information

ABSTRACT: The complexity of the mineral−organic carbon interface may influence the extent of stabilization of organic carbon compounds in soils, which is important for global climate futures. The nanoscale structure of a model interface was examined here by depositing films of organic carbon compounds of contrasting chemical character, hydrophilic glucose and amphiphilic stearic acid, onto a soil mineral analogue (Al_2O_3). Neutron reflectometry, a technique which provides depth-sensitive insight into the organization of the thin films, indicates that glucose molecules reside in a layer between Al_2O_3 and stearic acid, a result that was verified by water contact angle measurements. Molecular dynamics simulations reveal the thermodynamic driving force behind glucose partitioning on the mineral interface: The entropic penalty of confining the less mobile glucose on the mineral surface is lower than for stearic acid. The fundamental information obtained here helps rationalize how complex arrangements of organic carbon on soil mineral surfaces may arise.

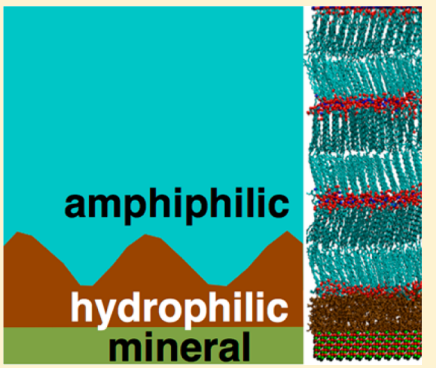

INTRODUCTION

Understanding the stabilization of soil organic matter (SOM), which represents the largest terrestrial carbon reservoir, is crucial in determining soil response to climate change.[1−3] The interaction of organic carbon with soil minerals is one of the main mechanisms of SOM stabilization. Heterogeneous mixtures of dissolved biopolymers derived from plants and microbes can adsorb to minerals and become stabilized for months to centuries.[4,5] Therefore, obtaining a detailed understanding of the organo−mineral interface is critical to comprehending stabilization mechanisms of organic compounds in soils.

Organic carbon in soils is a collection of relatively low molecular weight biopolymers derived from microbes and plants.[4,5] Recent models of the organic-mineral associations have proposed that layers of organic compounds form a discrete zonal sequence determined by the hydrophobicity of the compounds as well as other factors.[6−8] In these models, various functional groups on the SOM can bond or interact directly with hydroxyl groups on the mineral surfaces. Complex, multilayered structures can form when functional groups of new compounds attach directly to the mineral-associated compounds. For example, amphiphilic compounds having both a hydrophilic functional group and a hydrophobic portion may orient on the mineral and additional layers may also be formed by associations with the hydrophobic portions of the amphiphilic compounds.[6]

The importance of amphiphilic compounds in creating layers on a soil mineral surface was recently verified by neutron reflectometry (NR) studies.[9] Formation of distinct zones of compounds on a mineral surface was observed when an amphiphilic compound was mixed with natural organic matter.[9] In contrast, a single homogeneous layer was observed when a hydrophilic compound was introduced with natural organic matter.[9] These experiments are some of the first to interrogate the structure of layered organo−mineral interfaces, in part because there are only a limited number of techniques capable

Received: August 1, 2013
Revised: November 25, 2013
Accepted: December 2, 2013

 © XXXX American Chemical Society dx.doi.org/10.1021/es403430k | Environ. Sci. Technol. XXXX, XXX, XXX−XXX

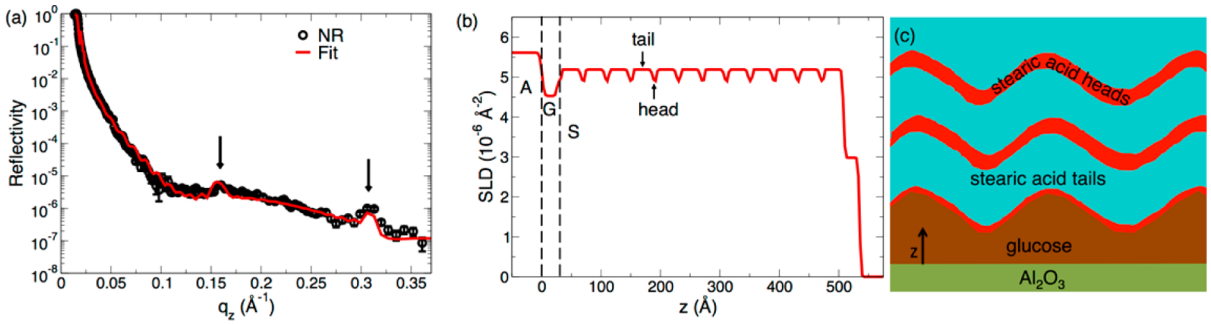

Figure 1. (a) Neutron reflectivity data of glucose and stearic acid on Al_2O_3 as a function of momentum transfer in the plane perpendicular to the Al_2O_3 layer. Experimental data are shown as symbols and the fit as a line. Bragg peaks due to the stacking arrangement of stearic acid bilayers are indicated by the arrows. (b) Scattering length density (SLD) profile as a function of the distance from the substrate obtained from fitting the experimental NR data of Figure 1a. Al_2O_3, glucose and stearic acid regions are labeled as A, G, and S respectively. Also indicated are the SLD of the tail and head regions of the stearic acid bilayers. (c) A schematic illustration of the proposed stacking and undulation of layers of organic material on Al_2O_3. The undulations lead to lateral heterogeneity in the sample.

of profiling the complex organization of organic materials on mineral surfaces at nanometer length-scales. As a result, the multilayer concept[6−8] lacks a set of governing principles supported by theoretical predictions and verified by experimentation. Thus, we are limited in our ability to infer the role of multilayered organo-mineral structures on carbon cycling in soils.

Our approach is to construct and study a simple organo−mineral model system that enables elucidation of the fundamental physicochemical interactions that are crucial in stabilizing organic carbon compounds in soils. We deposited onto sapphire (Al_2O_3), a representative soil mineral, two films of simple organic compounds differing in chemical character: first hydrophilic glucose was deposited, representative of sugars found in soil, and then stearic acid, representative of the amphiphilic molecules found in soil. The latter contains a long hydrophobic hydrocarbon tail and a hydrophilic carboxylic acid headgroup (depicted in Supporting Information (SI) Figure S1). The thickness, density, and nanoscale structure and composition of these films were studied using neutron reflectometry. A distinct zonal arrangement of the organic compounds was revealed, with the hydrophilic molecules forming contact with the mineral. Molecular dynamics (MD) simulations investigated thermodynamic contributions of the organic compounds stabilization on the mineral.

MATERIALS AND METHODS

Sample Preparation. We used C-plane, 2.5 cm diameter and one side polished sapphire (Al_2O_3) as a model soil mineral (MTI corporation), and glucose (Sigma Aldrich) and deuterated stearic acid (Cambridge Isotope Laboratories, Inc.) as model organic carbon (OC) compounds, see SI Figure S1. The glucose represents a hydrophilic compound and stearic acid represents a typical amphiphilic compound present in soil−organic matter. By deuterating only the tail component of stearic acid ($C_{17}D_{35}$), and not the head component (COOH), maximum contrast in neutron reflectivity signal between the tail and head parts of stearic acid was expected. Solutions of the compounds at a concentration of 1000 mg L^{-1} were prepared on the day of deposition on Al_2O_3 surface by dissolving glucose in pure Milli-Q (MQ) water and the deuterated stearic acid in toluene. Toluene was used as a solvent because its relatively high vapor pressure promotes evaporation upon deposition to form the sample, which results in smooth films. The scattering length density (SLD) found from previous neutron reflectometry (NR) measurements is consistent with no residual toluene.[9] These solutions were applied on plasma cleaned Al_2O_3 surfaces by spin coating.[9,10] Solutions of 300 μL were applied on the mineral substrate and the substrate was then rotated immediately at a speed of 1000 rpm for 45 s. In addition to preparing individual films of glucose and stearic acid on Al_2O_3 surface, a two-layer sample was prepared by coating both glucose and stearic acid in sequence on the mineral surface. The spin-coated samples were stored in a glovebox overnight under N_2 before neutron reflectivity measurements.

Neutron Reflectometry. Neutron reflectometry (see SI Figure S2) is commonly employed to study the structure of thin films[11] and is a well-suited technique for the interrogation of SOM model systems because of it subnanometer resolution, sensitivity to light elements and sensitivity to isotopes, which allows contrast to be selectively enhanced.[9] Here NR is employed to deduce changes in density and composition along the direction perpendicular to the mineral surface. The reflectivity data was collected using the NR instrument MAGICS at the Spallation Neutron Sources at the Oak Ridge National Laboratory.[12] It is a time-of-flight instrument with wavelength range of 2−5 Å. The SLD is a function of the scattering vector transfer perpendicular to the surface given as $q_z = 4\pi \sin\Theta/\lambda$, where λ is the neutron wavelength. The depth dependence of the SLD of the system in Figure 1 is obtained by model fitting the reflectivity data using the Parratt formalism for stratified homogeneous layers with different densities and thicknesses,[13] employing the software Parratt 32 (http://parratt32.software.informer.com/).

Contact Angle Measurement. Contact angle measurements were carried out using a KRÜSS DSA 30 contact angle goniometer equipped with a charge-coupled device (CCD) camera. Al_2O_3 wafers coated with the organic compounds were mounted on the goniometer stage and a single drop (5 μL) of MQ water was dispensed on the sample surface using the automated liquid handling controls of the instrument. The drop was allowed to reach equilibrium before recording the shape, from which the contact angle was determined. The measurement was conducted at five locations on each sample and the mean contact angle and standard error per sample are reported.

Molecular Dynamics Simulations. Molecular Dynamics (MD) simulations are commonly employed to study the structure and dynamics of biomolecules and have been recently applied to plant biopoylmers[14] and organo-mineral interfaces.[15,16] Here MD simulations were performed on five systems:

dx.doi.org/10.1021/es403430k | Environ. Sci. Technol. XXXX, XXX, XXX−XXX

stearic acid/glucose/Al_2O_3 (Figure 2); bulk stearic acid (SI Figure S3c); stearic acid/Al_2O_3 (SI Figure S3d); glucose/Al_2O_3

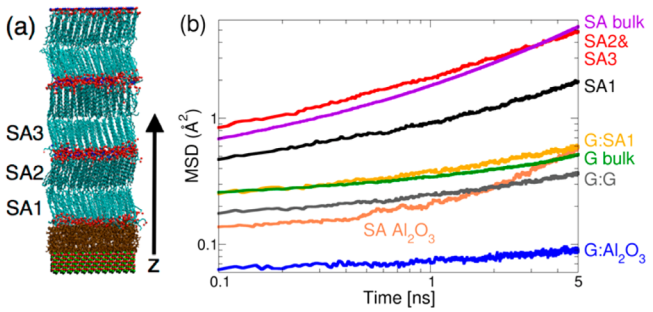

Figure 2. (a) Snapshot of the simulation of stearic acid (oxygen in red, carbon in cyan) and glucose (brown) deposited on Al_2O_3 (oxygen in red and aluminum in green). Stearic acid layers SA1, SA2, and SA3 are also identified. (b) Mean-square displacement as a function of time for the following types of molecules: stearic acid layer SA1 (SA1); stearic acid layers SA2 and SA3 (SA2 & SA3); bulk stearic acid (SA bulk), derived from a separate simulation; stearic acid on Al_2O_3 surface in the absence of glucose (SA:Al_2O_3) derived from a separate simulation, see SI Figure S3e; glucose in contact with stearic acid (G:SA1); glucose in contact with Al_2O_3 (G:Al_2O_3); glucose in contact only with other glucose molecules (G:G); bulk glucose (G bulk), derived from a separate simulation.

(SI Figure S5a) and bulk glucose (not shown). The NAMD 2.9 software[17] was used employing the CHARMM carbohydrate force field[18] for glucose and lipid force field[19] for stearic acid, which was protonated as its pK_a~10.[20]The partial charge for Al atom is +2.78e, and for the O atom is −1.85e.[21] The Lennard-Jones parameters for Al_2O_3 were obtained from the force field in ref 21., which also was used previously to study the absorption of alkenes on Al_2O_3.[22] Periodic boundary conditions were employed with the Particle Mesh Ewald method[23] with grid spacing of 1.2 Å for the treatment of Coulomb interactions beyond 11 Å and a force switching function to smoothly transition the Lennard-Jones forces to zero over the range of 10−11 Å. Multiple time step integration was used with timesteps of 2 fs for bonded and short-range nonbonded forces, and 4 fs for the long-range electrostatic forces. The neighbor list was updated every 10 steps with a pair-list distance of 12.5 Å. The SHAKE algorithm[24] was used to constrain all covalent bonds involving hydrogen atoms to their equilibrium values. The Al_2O_3 atoms were restrained to their crystallographic positions and the simulations were performed in the NVT ensemble. In all simulations, the density of glucose was 1.51 g/cm^3 (c.f. nominal density of 1.55 g/cm^3), and that of stearic acid 1.07 g/cm^3 (c.f. nominal density of 1.02 g/cm^3). The temperature was kept constant using the Langevin dynamics algorithm implemented in X-PLOR with a damping coefficient of 5 ps^{-1}. All simulations were of 25 ns length each.

■ RESULTS AND DISCUSSION

The specular NR data from glucose and stearic acid deposited on a thin slab of Al_2O_3 are shown in Figure 1a. The form of the NR curve is determined by the variation of the neutron scattering length density (SLD) along z, the direction perpendicular to the mineral surface. The experimental reflectivity data show a signature feature—Bragg peaks at ~0.16 and ~0.32 Å^{-1}, highlighted by the arrows in Figure 1a − that indicates repeating layers on the sample. The value of momentum transfer q_z of the Bragg peak is inversely proportional to the average thickness D of the repeating structure $q_z = 2\pi/D$, and the peak height is related to the number of layers stacked on top of each other. Selective perdeuteration of the hydrophobic tail of stearic acid was used to distinguish the hydrophobic tail region from the hydrophilic carboxylic acid functional group (SI Figure S1). By constructing a model to fit the data, we infer that the amphiphilic stearic acid molecules A-B (where A stands for the $C_{17}D_{35}$ hydrophobic tail and B for the COOH hydrophilic head) were self-assembled into a repeating structure B-A-A-B (SI Figure S1) that may be considered "classical" for stratified amphiphilic systems.[25] The Bragg peaks are also observed in a control experiment using a single film of stearic acid deposited on Al_2O_3 (in the absence of glucose), shown in SI Figure S3, supporting that the Bragg peaks are indeed associated with stearic acid. In contrast, no Bragg peaks are associated with glucose films on Al_2O_3 (SI Figure S4). Stearic acid has also been observed previously to form self-assembled bilayers on aluminum oxide surfaces.[25]

To determine the locations of the compounds on the mineral surface, the NR data were modeled using a three-layer structure atop Al_2O_3 consisting of glucose and a stack of stearic acid bilayers made of the BAAB repeating structure of the perdeuterated hydrophobic tails ($C_{17}D_{35}$) and the hydrophilic head groups (COOH). The SLD of the hydrophobic tails and the hydrophilic heads, as well as the different compounds, are sufficiently unique as to permit identification when occurring together in a single sample.[9] The order of layer stacking, the thickness and SLD of each layer and the number of stearic acid bilayers were varied in order to best reproduce the NR data (Figure 1b). The total thickness of the repeating layer as obtained from the first Bragg peak is ~40 Å (SI Figure S1). The layer of stearic acid head groups (BB) are found to have a thickness of 7.5 Å and a SLD of 4.9 × 10^{-6} Å^{-2}, which is larger than the nominal SLD of a COOH group (SLD = 2.0 × 10^{-6} Å^{-2}). The strata of tails (AA) are found to have a thickness of 32.8 Å and SLD of 5.2 × 10^{-6} Å^{-2}, which is smaller than the SLD value predicted for $C_{17}D_{35}$ (SLD = 7.7 × 10^{-6} Å^{-2}).

The deviation of the measured SLD from nominal values is interpreted as arising from lateral undulation of the bilayers,[26] which has been previously reported for stearic acid thin films.[27] The presence of undulation leads to heterogeneity in the lateral dimension of the bilayer, i.e. perpendicular to z, so that, at a particular distance from the mineral surface, both head groups and tails of stearic acid can be found at slightly different depths in the sample as a function of lateral position (Figure 1c). Because specular reflectivity measures the laterally averaged structure (SLD) in the plane of the film, the strata nominally assigned as "head"- or "tail"-containing regions have some overlap of COOH and $C_{17}D_{35}$ moieties. Similar stearic acid undulations were inferred when stearic acid was deposited on Al_2O_3 in the absence of glucose (SI Figure S3).

The derived SLD profiles in Figure 1b show a 25 Å thin layer with an SLD of 4.5 × 10^{-6} Å^{-2} on the Al_2O_3 surface. The observed SLD is greater than the nominal value of glucose (SLD = 1.5 × 10^{-6} Å^{-2}). We interpret this SLD as originating from a thin (≤25 Å) glucose film found on the mineral surface, whose thickness varies due to the stearic acid undulations (Figure 1c).

Previous NR experiments on a sample where stearic acid was deposited first to Al_2O_3 followed by glucose, that is, the order of deposition was the opposite of the one reported here, also found glucose to partition on the mineral surface. This suggests that the final spatial arrangement of the glucose and stearic acid

dx.doi.org/10.1021/es403430k | Environ. Sci. Technol. XXXX, XXX, XXX−XXX

layers is independent of their initial order of deposition on Al_2O_3 and that glucose being found on the mineral surface is the thermodynamically favored state of this system. The relatively small thickness of the glucose layer compared to stearic acid is in agreement with sorption experiments of glucose and stearic acid performed on soil minerals, which find that more stearic acid sorbs to Al_2O_3 than glucose.[28]

In order to provide additional support to our interpretation that glucose contacts the Al_2O_3 substrate and that stearic acid segregates to the air interface, water contact angles were measured to characterize the wetting characteristics of three systems. When both stearic acid and glucose were deposited on Al_2O_3, the contact angle ($\phi_{GS} = 69 \pm 5°$) was similar to when Al_2O_3 was covered with only stearic acid ($\phi_S = 68 \pm 9°$). These values are very different from when only glucose was deposited on the mineral surface ($\phi_G = 24 \pm 6°$), thus providing additional support of our interpretation of the spatial arrangement of the compounds observed from the NR experiments. Further, the same spatial arrangement of glucose and stearic acid also was found when these organic compounds were deposited on a rough alumina surface.[9]

Molecular dynamics simulations were performed to corroborate the model obtained from fitting the NR and to obtain atomic-level understanding of the thermodynamics of adsorption to minerals and how association between molecules at interfaces alters their dynamics and order. A model system consisting of three stearic acid bilayers and a glucose slab stacked on an Al_2O_3 surface (Figure 2a) was used. During the simulation, the Al_2O_3 atoms were fixed to their crystallographic positions and the temperature and volume of the system were held constant.

In order to determine why glucose, rather than stearic acid, was found at the film/mineral interface, two separate simulations were performed: glucose was deposited on Al_2O_3 and stearic acid was deposited on Al_2O_3 (SI Figures S3d, S5a). The mean square displacement (MSD) of each molecule, which is a measure of its mobility,[29] was calculated from a simulation mimicking the experimental system, where glucose and stearic acid were deposited on Al_2O_3 (see Figure.2a):

$$\mathrm{MSD}(t) = \langle [r(t) - r(0)]^2 \rangle \quad (1)$$

where $r(t)$ is the position of a molecule at time t. Departure from linearity at time lags >0.5 ns is due the fact that MSD points are less averaged, thus resulting in large statistical fluctuations.[30] This is particularly evident in the rapid rise of the MSD of SA:Al_2O_3 for $t > 1$ *ns*

Figure 2b shows that the glucose molecules on the Al_2O_3 interface show a significant retardation in their dynamics, with the MSD after 5 ns being about five times smaller compared to the MSD of glucose in the bulk. Confinement to the interface leads to the retardation, compared to molecules in a bulk system or to molecules in the middle of the glucose slab away from the substrate. On the other hand, glucose molecules on the interface with stearic acid, which is more mobile than glucose, show slightly faster dynamics than bulk. We also find that the mobility of the first layer of stearic acid layer in contact with glucose (SA1, as seen in Figure 2a) is lower than when it is in the bulk. The MSD of stearic acid molecules in contact with itself is similar to that of bulk. This set of findings suggest that a mineral:glucose interface is entropically more favorable than a mineral:stearic acid interface. The organic carbon molecules in contact with the mineral surface are immobilized due to confinement. Therefore, the entropic penalty resulting from confinement is lower for glucose because its bulk mobility is lower than that of stearic acid.

To probe how the interfaces influence the orientational order of glucose and stearic acid, an order parameter P:

$$P = \left\langle \frac{3\cos^2\theta - 1}{2} \right\rangle \quad (2)$$

is computed, where θ is the angle between the z-axis, which is perpendicular to the surface plane of the mineral (Figure 2a) and vector **n**, which defines a molecular axis. **n** is defined for glucose as normal to the plane of the glucose ring and for stearic acid as connecting its headgroup to the end of its tail (SI Figure S1). A completely isotropic arrangement of the molecules has $P = 0$ whereas a perfectly aligned sample, where all vectors **n** are parallel to the z-axis, results in $P = 1$. Glucose molecules that are in contact with stearic acid are slightly less orientationally ordered ($P = 0.10 \pm 0.05$) than those that are in contact only with other glucose molecules ($P = 0.18 \pm 0.03$). However, contact with Al_2O_3 does not significantly change the orientational order of glucose ($P = 0.13 \pm 0.06$). Stearic acid molecules in the layer that is in contact with glucose (layer SA1) are less ordered ($P = 0.42 \pm 0.04$) than those molecules in layers SA2 and SA3, which are in contact only with each other ($P = 0.55 \pm 0.02$). Therefore, the orientational order of only stearic acid is influenced significantly by the interface with glucose, whereas that of glucose remains unaffected by the interfaces with stearic acid and Al_2O_3.

A molecular-level description of the sorptive behavior of glucose on the mineral is provided by the relative small value of P, which indicates that glucose rings are mostly not parallel to the mineral surface. This orientational behavior indicates that stacking interactions, which would lead to parallel orientations on the mineral surface, are not as dominant as interactions between the glucose hydroxyl groups and the mineral. The latter interactions do not necessarily lead to planar orientations, see SI Figure S5b. In contrast to glucose, aromatic compounds can sorb to minerals in highly parallel orientations due to $n-\pi$ interactions between the nonbonding electrons at siloxane surfaces and aromatic π electrons.[31]

In summary, models of the organic-mineral interface in soils postulate that organic compounds form a discrete zonal sequence determined by their hydrophobicity.[5−8] The nanoscale investigation of the spatial heterogeneity of soil organic matter provides substantial experimental challenges in terms of resolution and depth-sensitivity. We have constructed a simple model system of Al_2O_3, glucose molecules, representative of hydrophilic sugars in SOM and stearic acid, which represents simple amphiphilic carbon compounds found in SOM. Although this model system does not mimic the complexity of soil organic matter, it does capture the fundamental physicochemical interactions between a mineral and organic molecules of contrasting hydrophobicity

Our neutron reflectivity and water contact angle measurements not only confirm the presence of discrete zones, but also determine the spatial order of compounds in this zonal structure. Glucose molecules arranged in a thin film between the Al_2O_3 mineral and stearic acid,.Atomistic molecular dynamics simulations suggest that the thermodynamic driving force behind glucose partitioning on the mineral surface arises from the entropic penalty of confining the less mobile glucose on the mineral surface is lower than for stearic acid. The simulations further demonstrate how interfaces affect the

dynamic and orientational properties of the organic molecules. Although the mineral interface slows the dynamics of glucose compared to bulk, the orientational order of glucose molecules is not affected significantly. On the other hand, the glucose:stearic acid interface slows the dynamics and reduces the orientational order of the stearic acid.

Our integrated experimental and computational studies thus propose a detailed understanding of how physicochemical influences of the environment could allow easily degradable sugars to persist in SOM with long residence times.[1] The fundamental information provided here helps to probe the structure of the environmentally important organo−mineral interface in soils at the nanoscale and rationalize the complex spatial arrangement of organic compounds.

■ ASSOCIATED CONTENT

Supporting Information

Schematic of the scheme used to fit the NR data (Figure S1). Description of NR technique; NR results of stearic acid deposited on Al_2O_3; NR and MD results of glucose deposited on Al_2O_3. This material is available free of charge via the Internet at http://pubs.acs.org.

■ AUTHOR INFORMATION

Corresponding Author

*Phone:+1-865-576-2576; e-mail: petridisl@ornl.gov.

Notes

The authors declare no competing financial interest.

■ ACKNOWLEDGMENTS

This project is funded by the Oak Ridge National Laboratory (ORNL) Director's Research and Development Program (LDRD). Research at the ORNL Spallation Neutron Source was sponsored by the Scientific User Facilities Division, Office of Basic Energy Sciences (BES), U.S. Department of Energy (DOE). A portion of this research was conducted at ORNL's Center for Nanophase Materials Sciences, which is sponsored by the Scientific User Facilities Division of BES at DOE. ORNL is managed by UT-Battelle, LLC, under contract DE-AC05-00OR22725 with the DOE. This work used the Extreme Science and Engineering Discovery Environment (XSEDE), which is supported by National Science Foundation grant number OCI-1053575.

■ REFERENCES

(1) Schmidt, M. W. I.; Torn, M. S.; Abiven, S.; Dittmar, T.; Guggenberger, G.; Janssens, I. A.; Kleber, M.; Kogel-Knabner, I.; Lehmann, J.; Manning, D. A. C.; Nannipieri, P.; Rasse, D. P.; Weiner, S.; Trumbore, S. E. Persistence of soil organic matter as an ecosystem property. *Nature* **2011**, *478* (7367), 49−56.

(2) von Lutzow, M.; Kogel-Knabner, I.; Ekschmitt, K.; Matzner, E.; Guggenberger, G.; Marschner, B.; Flessa, H. Stabilization of organic matter in temperate soils: Mechanisms and their relevance under different soil conditions—A review. *Eur. J. Soil Sci.* **2006**, *57* (4), 426−445.

(3) Mikutta, R.; Schaumann, G. E.; Gildemeister, D.; Bonneville, S.; Kramer, M. G.; Chorover, J.; Chadwick, O. A.; Guggenberger, G. Biogeochemistry of mineral-organic associations across a long-term mineralogical soil gradient (0.3−4100 kyr), Hawaiian Islands. *Geochim. Cosmochim. Acta* **2009**, *73* (7), 2034−2060.

(4) Kelleher, B. P.; Simpson, A. J. Humic substances in soils: Are they really chemically distinct? *Environ. Sci. Technol.* **2006**, *40* (15), 4605−4611.

(5) Sutton, R.; Sposito, G. Molecular structure in soil humic substances: The new view. *Environ. Sci. Technol.* **2005**, *39* (23), 9009−9015.

(6) Kleber, M.; Sollins, P.; Sutton, R. A conceptual model of organo-mineral interactions in soils: Self-assembly of organic molecular fragments into zonal structures on mineral surfaces. *Biogeochemistry* **2007**, *85* (1), 9−24.

(7) Wershaw, R. L. A new model for humic materials and their interactions with hydrophobic organic chemicals in soil-water or sediment-water systems. *J. Contam. Hydrol.* **1986**, *1* (1−2), 29−45.

(8) Wershaw, R. L. Model for humus in soils and sediments. *Environ. Sci. Technol.* **1993**, *27* (5), 814−816.

(9) Mayes, M.; Jagadamma, S.; Ambaye, H.; Petridis, L.; Lauter, V. Neutron reflectometry reveals the internal structure of organic compounds deposited on aluminum oxide. *Geoderma* **2013**, *192*, 182−188.

(10) Wang, Y. M.; Wang, P.; Kohls, D.; Hamilton, W. A.; Schaefer, D. W. Water absorption and transport in bis-silane films. *Phys. Chem. Chem. Phys.* **2009**, *11* (1), 161−166.

(11) Kirby, B. J.; Kienzle, P. A.; Maranville, B. B.; Berk, N. F.; Krycka, J.; Heinrich, F.; Majkrzak, C. F. Phase-sensitive specular neutron reflectometry for imaging the nanometer scale composition depth profile of thin-film materials. *Curr. Opin. Colloid Interface Sci.* **2012**, *17* (1), 44−53.

(12) Lauter, V.; Ambaye, H.; Goyette, R.; Lee, W. T. H.; Parizzi, A. Highlights from the magnetism reflectometer at the SNS. *Phys. B, Condensed Matter* **2009**, *404* (17), 2543−2546.

(13) Parratt, L. G. Surface studies of solids by total reflection of X-rays. *Phys. Rev.* **1954**, *95* (2), 359−369.

(14) (a) Bellesia, G.; Chundawat, S. P. S.; Langan, P.; Dale, B. E.; Gnanakaran, S. Probing the early events associated with liquid ammonia pretreatment of native crystalline cellulose. *J. Phys. Chem. B* **2011**, *115* (32), 9782−9788. (b) Petridis, L.; Schulz, R.; Smith, J. C. Simulation analysis of the temperature dependence of lignin structure and dynamics. *J. Am. Chem. Soc.* **2011**, *133* (50), 20277−20287. (c) Mazeau, K.; Charlier, L. The molecular basis of the adsorption of xylans on cellulose surface. *Cellulose* **2012**, *19* (2), 337−349.

(15) Sutton, R.; Sposito, G. Molecular simulation of humic substance-Ca-montmorillonite complexes. *Geochim. Cosmochim. Acta* **2006**, *70* (14), 3566−3581.

(16) Teppen, B. J.; Yu, C. H.; Miller, D. M.; Schafer, L. Molecular dynamics simulations of sorption of organic compounds at the clay mineral aqueous solution interface. *J. Comput. Chem.* **1998**, *19* (2), 144−153.

(17) Phillips, J. C.; Braun, R.; Wang, W.; Gumbart, J.; Tajkhorshid, E.; Villa, E.; Chipot, C.; Skeel, R. D.; Kale, L.; Schulten, K. Scalable molecular dynamics with NAMD. *J. Comput. Chem.* **2005**, *26* (16), 1781−1802.

(18) Guvench, O.; Greene, S. N.; Kamath, G.; Brady, J. W.; Venable, R. M.; Pastor, R. W.; Mackerell, A. D. Additive empirical force field for hexopyranose monosaccharides. *J. Comput. Chem.* **2008**, *29* (15), 2543−2564.

(19) Feller, S. E.; Gawrisch, K.; MacKerell, A. D. Polyunsaturated fatty acids in lipid bilayers: Intrinsic and environmental contributions to their unique physical properties. *J. Am. Chem. Soc.* **2002**, *124* (2), 318−326.

(20) Kanicky, J. R.; Shah, D. O. Effect of degree, type, and position of unsaturation on the pK(a) of long-chain fatty acids. *J. Colloid Interface Sci.* **2002**, *256* (1), 201−207.

(21) Ruberto, C.; Yourdshahyan, Y.; Lundqvist, B. I. Surface properties of metastable alumina: A comparative study of κ- and α-Al_{2}O_{3}. *Phys. Rev. B* **2003**, *67* (19), 195412.

(22) Li, C.; Choi, P. Molecular dynamics study of the adsorption behavior of normal alkanes on a relaxed α-Al2O3 (0001) surface. *J. Phys. Chem. C* **2007**, *111* (4), 1747−1753.

(23) (a) Darden, T.; York, D.; Pedersen, L. Particle mesh Ewald—An N logN method for Ewald sums in large systems. *J. Chem. Phys.* **1993**, *98* (12), 10089−10092. (b) Essmann, U.; Perera, L.; Berkowitz, M. L.;

504 Darden, T.; Lee, H.; Pedersen, L. G. A smooth particle mesh Ewald
505 method. *J. Chem. Phys.* **1995**, *103* (19), 8577−8593.
506 (24) Ryckaert, J. P.; Ciccotti, G.; Berendsen, H. J. C. Numerical
507 integration of cartesian equations of motion of a system with
508 constraints- molecular dynamics of *n*-alkanes. *J. Comput. Phys.* **1977**,
509 *23* (3), 327−341.
510 (25) Wiesler, D. G.; Feigin, L. A.; Majkrzak, C. F.; Ankner, J. F.;
511 Berzina, T. S.; Troitsky, V. I. Neutron and X-ray reflectivity study of Ba
512 salts of alternating bilayers of deuterated and hydrogenated stearic
513 acid. *Thin Solid Films* **1995**, *266* (1), 69−77.
514 (26) Nagle, J. F.; Tristram-Nagle, S. Structure of lipid bilayers. *BBA,*
515 *Biochim. Biophys. Acta, Rev. Biomembr.* **2000**, *1469* (3), 159−195.
516 (27) Nakayama, T.; Gemma, N.; Miura, A.; Azuma, M. Direct
517 observation of the surface structure of Languimir-Blodgett films with
518 scanning electron microscopy. *Thin Solid Films* **1989**, *178*, 477−481.
519 (28) Jagadamma, S.; Mayes, M. A.; Zinn, Y. L.; Gísladóttir, G.;
520 Russell, A. E. Sorption of organic carbon compounds to the fine
521 fraction of surface and subsurface soils. *Geoderma* **2014**, *213* (0), 79−
522 86.
523 (29) (a) Knight, J. D.; Lerner, M. G.; Marcano-Velazquez, J. G.;
524 Pastor, R. W.; Falke, J. J. Single molecule diffusion of membrane-
525 bound proteins: Window into lipid contacts and bilayer dynamics.
526 *Biophys. J.* **2010**, *99* (9), 2879−2887. (b) Petridis, L.; Pingali, S. V.;
527 Urban, V.; Heller, W. T.; O'Neil, H. M.; Foston, M.; Ragauskas, A.;
528 Smith, J. C., Self-similar multiscale structure of lignin revealed by
529 neutron scattering and molecular dynamics simulation. *Phys. Rev. E*
530 **2011**, *83* (6).
531 (30) Michalet, X. Mean square displacement analysis of single-
532 particle trajectories with localization error: Brownian motion in an
533 isotropic medium. *Phys. Rev. E* **2010**, *82* (4), 041914.
534 (31) Keiluweit, M.; Kleber, M. Molecular-level interactions in soils
535 and sediments: The role of aromatic pi-systems. *Environ. Sci. Technol.*
536 **2009**, *43* (10), 3421−3429.